Time Dependent Gating in Nanochannels

Caitlin Boone – Hayes Forum 2016

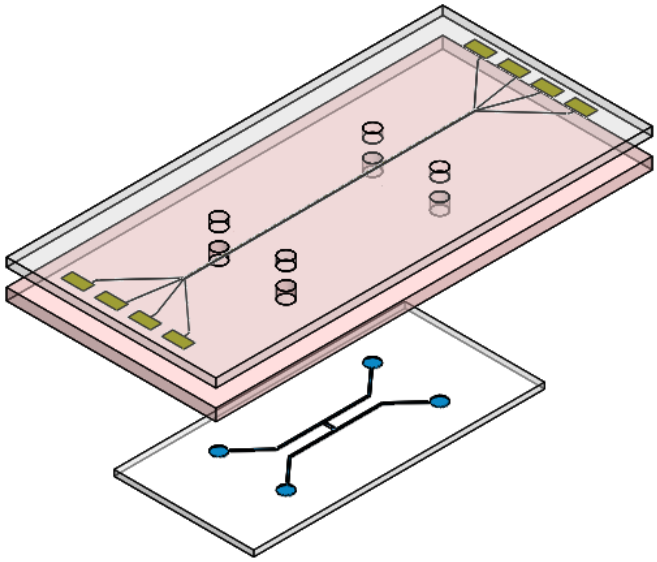

Figure 1: The nanofluidic field effect device used in this study. The top cover houses four embedded gate electrodes. Only one gate electrode was active at any given time. The polydimethylsiloxane (PDMS) layer insulates the gate electrodes fluidically and electrically from the nanochannels and is shown here in pink. The bottom channel slide has 2 microchannels connected to 4 fluidic reservoirs with a bank of three nanochannels running between the microchannels.

A device incorporating a nanochannel is said to have at least one critical dimension that measures between 1 and 100 nm. Typically, this critical dimension is the depth of the nanofluidic channel. Nanofluidic field effect devices, geometrically analogous to semiconductor based field effect transistors, feature a gate electrode embedded in the wall of the nanofluidic channel, electrically and fluidically isolated from the working fluid. An example is shown in Figure 1. Inside the nanochannel, the entire depth of the channel is affected by the surface charge of the walls around the channel. For glass devices with a pH 7 electrolyte solution, this means the channel walls are negatively charged. The gate electrode housed in the top cover of the device generates a local change in the effective surface charge of the nanochannel wall directly beneath the gate. The change in surface charge alters the electric field, likely extending throughout the depth of the nanochannels (M. Fuest, Boone, Rangharajan, Conlisk, & Prakash, 2015), allowing for the manipulation of the potential at the dielectric-electrolyte interface (M. Fuest, et al., 2015; W Guan, Fan, & Reed, 2011; Karnik et al., 2005). To

Adviser: Shaurya Prakash
Collaborators: Marie Fuest and Kyle Wellmerling

satisfy electroneutrality, this necessitates that the balance of ions inside the nanochannel must be altered to account for this change in effective surface charge. This allows for active, tunable control of ionic transport through the nanochannel. Control over ionic transport through nanofluidic devices is desired for a wide range of applications including water desalination (Kim, Ko, Kang, & Han, 2010; Shannon, 2010), "smart drug delivery" (R. Duan, Xia, & Jiang, 2013), ion separation (Kim, et al., 2010), DNA sequencing (Ai, Zhang, & Qian, 2010; Xia, Yan, & Hou, 2012), biosensing applications (C. Duan & Majumdar, 2010; Huo, Guo, & Jiang, 2011; Karnik, et al., 2005; Wei, Gatterdam, Wieneke, Tampé, & Rant, 2012), single molecule sensors (Howorka & Siwy, 2009), energy conversion (Siria et al., 2013; W Sparreboom, van den Berg, & Eijkel, 2010), and more.

To begin implementing devices for these applications, three main goals must be met:

1. Control the flow of with "gating" (starting and stopping transport)
2. Preferential transport of ions
3. Control of fluid flow direction

(R. Duan, et al., 2013 ; Hille, 2001; Huo, et al., 2011; Liu et al., 2014). Many advances have been made toward these goals in nanochannels. With various potentials applied to the gate electrodes, the devices used in this work has been shown to create a three state switch that can change the net direction of current moving through the nanochannels by altering the applied gate electrode (M. Fuest, et al., 2015). This directly addresses the first of the three goals. Additionally, this device has been used to study ionic transport characteristics using 4 distinct ions (K^+, Na^+, Ca^{2+}, and Mg^{2+}) for at a range of pHs (2-10) making a step toward preferential transport (M. Fuest, Boone, Rangharajan, Conlisk, & Prakash, 2016) by characterizing the differences in transport through the channel. Working toward the third of the three goals, in microchannels, previous reports have

Adviser: Shaurya Prakash
Collaborators: Marie Fuest and Kyle Wellmerling

shown when a flow is driven by an AC voltage source, the applied frequency can alter the direction of fluid flow (Martin Z. Bazant et al., 2007; Garcia-Sanchez, Ramos, Green, & Morgan, 2006; Lastochkin, Zhou, Wang, Ben, & Chang, 2004; Storey, Edwards, Kilic, & Bazant, 2008; Vincent Studer, Pépin, Chen, & Ajdari, 2004; Urbanski, Thorsen, Levitan, & Bazant, 2006; Yang, Jiang, & Ramos, 2009). Our work focuses on using an alternating current to generate the gate excitation; a rarely explored parameter in these devices.

Aside from a few notable exceptions covered below, existing literature seems to lack modeling or experimental research using a gate electrode with applied AC potentials as opposed to the traditionally used DC signals. This has been studied extensively in microchannels with promising results though it should be emphasized that not all effects seen in microchannels translate into effects in nanochannels. In microchannels, using AC signals applied to the gate electrode, it was proposed that a series of AC driven gate electrodes could create a series of vortices that would drive flow through a microchannel (Ramos, Morgan, Green, & Castellanos, 1999) analogous to how a conveyer belt would move objects (M. Z. Bazant & Ben, 2006). This theory was shown to have a net pumping direction and first experimentally tested by Ajdari (Ajdari, 2000). These types of devices are called "ACEO pumps" meaning they are driven by alternating current electro-osmotic flow. For these gated ACEO devices, it has already been shown that fluid flow direction can be manipulated and reversed by altering the frequency of applied AC signals (Martin Z. Bazant et al., 2007; Garcia-Sanchez, Ramos, Green, & Morgan, 2006; Lastochkin, Zhou, Wang, Ben, & Chang, 2004; Storey, Edwards, Kilic, & Bazant, 2008; Studer, Pépin, Chen, & Ajdari, 2004; Urbanski, Thorsen, Levitan, & Bazant, 2006; Yang, Jiang, & Ramos, 2009) and to product higher measured current for the same equivalent applied voltages (Studer, et al., 2004). The devices typically used for these experimental studies have an array of gate electrodes, like the

device proposed by Ramos *et al.* (Ramos, et al., 1999) and originally implemented by Ajdari (Ajdari, 2000) and are used for low (<10 mM) concentrations of KCl (Martin Z. Bazant, Kilic, Storey, & Ajdari, 2009).

The frequency dependent pumping action seen in ACEO devices becomes almost non-existent for high salt concentrations (typically above 10 mM) (Martin Z. Bazant, et al., 2007; Soni, Squires, & Meinhart, 2007; Studer, et al., 2004; van der Wouden, Hermes, Gardeniers, & van den Berg, 2006) which is well below physiological concentrations (Huang, Bazant, & Thorsen, 2009) and the observed flow reversals have yet to be completely explained (Martin Z. Bazant, et al., 2009). This flow reversal has been attributed to bulk Joule heating (Garcia-Sanchez, et al., 2006) or Faradic reactions (Lastochkin, et al., 2004) due to bubbles appearing in the AC driven solutions but no simulations have matched these results. A single "characteristic frequency" related to the rate of double layer charging and discharging that would yield the highest velocity of fluid through the microchannel is believed to exist (Brown, Smith, & Rennie, 2000; Ramos, González, Castellanos, Green, & Morgan, 2003; Yang, et al., 2009). Deviation from this frequency would cause reduced fluidic flow through the microchannels.

The limited work that has been gone on AC gated nanofluidic channels has shown some frequency dependence when an array of electrodes was used but no work has been done with a single electrode. However, this work has never been attempted in gated nanofluidic channels aside from a brief experimental study into AC electroosmotic flow in 50 nm deep nanochannels (van den Beld, Sparreboom, van den Berg, & Eijkel, 2014) inspired by similar studies in microchannels. This study used an array of 100 gate electrode pairs and filled the device with a 100 μM solution of KNO_3. Only a sinusoidal signal was used over a 10 – 1000 Hz frequency range in this work looking at the impedance to try to characterize effects on velocity. In the end, it is noted that the

flow direction is opposite what was previously seen by Brown et al. (Brown, et al., 2000) in microchannels.

The second experimental study by Sparreboom et al. (Wouter Sparreboom, Cucu, Eijkel, & Berg, 2008) demonstrates a 50 nm deep nanochannel with flow driven by and electrode array with an applied 10 Hz signal. A concentration gradient across the device gives the device something to pump against with one reservoir holding 20 µm KNO_3 and the other holding 100 µm KNO_3. This conference paper points out again the clear lack of experiments or simulations related to AC gated nanofluidic channels and in the end shows the simulated currents through the device to be considerably short of the experimental values.

In addition to these experimental studies using a sinusoidal waveform at the gate, it has been predicted that for frequencies 1 Hz and below, nanofluidic devices will essentially be in quasi-steady state with the devices able to reach ionic equilibrium before the applied voltage signal switches (Weihua Guan & Reed, 2012). Outside of this work, much of what effects seen in AC gated microchannels will translate to the nanoscale remains unclear. Until this work, no experimental studies had been conducted with a device using only a

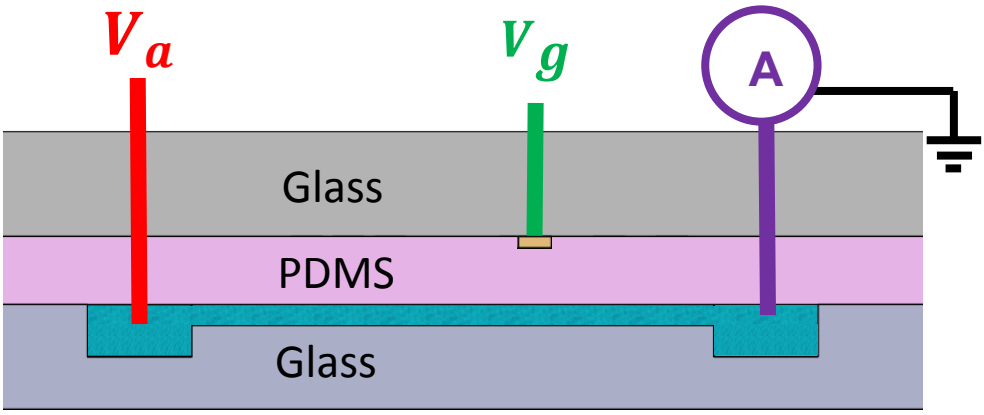

Figure 2: A cross section of the device showing the axial potential (V_a), the gate potential (V_g), and the measured current (shown through the ammeter). Both function generators required to generate the gate and axial potentials share a common ground with the picoammeter. The physical measurement takes place in an Earth grounded Faraday cage to eliminate electrical interference.

single gate electrode as is common in DC gated devices. Additionally, for the first time an AC signal is directly compared to the commonly used DC signal. The frequency range explored in this work, while narrow, also represents the first time the effect of multiple frequencies have been compared to one another in terms of effects on measured current in a nanofluidic device.

Here, the experiments were conducted with a nanofluidic field effect device filled with a 1 mM potassium chloride electrolyte solution at pH 7. No concentration gradient was added to the system. The nanofluidic channels were 16 nm deep x 30 μm wide x 2 mm long and the two microchannels were 10 μm deep x 50 μm wide x and 3 cm long. The device top cover housing 4 individually addressable gate electrodes and channel slide were fabricated through a wet etching and UV photolithography process summarized in Figure 3. Monovalent potassium chloride (KCl) was the primarily used electrolyte with deionized water used for initial device characterization. Axial (applied across the nanochannels, V_a) and gate (applied to the gate electrode, V_g) voltages were applied to systematically explore the effect of the gate electrode on the ionic transport in the nanochannels as measured through the ionic current measured through the device. Both DC and root mean square (RMS) matched AC signals were applied to the gate electrode and compared the results were analyzed and compared for time averaged current, total change in the current or "current modulation", and average charge through the nanochannels in a given time period.

Using a set of standard runs for a range of axially applied DC current (V_a) the current (I), the measured intrinsic conductance (g) is then calculated using

$$g = I/V_a \qquad \text{[Equation 1]}$$

Adviser: Shaurya Prakash
Collaborators: Marie Fuest and Kyle Wellmerling

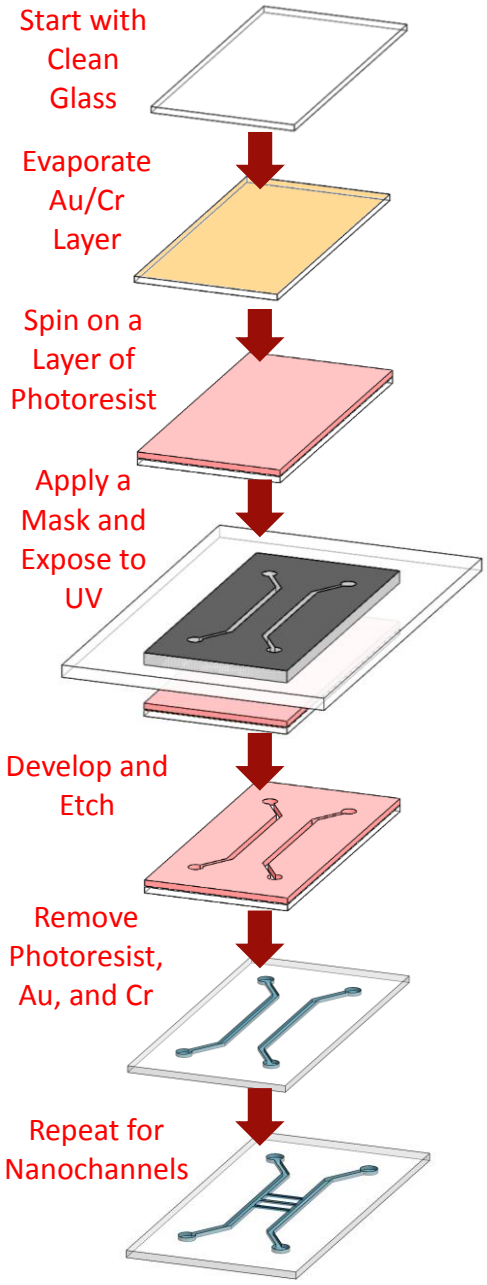

Figure 3: A summary of the fabrication steps used to create the channel slides. A variation of this process is used for the device top covers.

and compared to previous devices (M. J. Fuest, 2016; W Guan, et al., 2011). The original idea to use conductance as a tool to compare device was inspired by the conductance measurements used to compare solid state FETs due to the extensive similarities between the 2 systems. Additionally, conductance describes the number of charge carriers in the channel allowing for analysis to determine the approximate channel dimensions (Stein, Kruithof, & Dekker, 2004).

The ability to establish the finished device geometry without breaking the device for an scanning electron microscope (SEM) image is extremely important because it determines if a given set of devices are near enough within experimental error to directly compare results to one another. If studying multiple ion types (a divalent vs. a monovalent for example), this is needed since the same device cannot be used for both electrolyte types. To do the initial match between devices, DI water was used as the working electrolyte and the devise are run through identical tests sweeping the axial voltage between 5 and -5 V DC. Typically, the amount of allowable error to call 2 devices

"DI Matched" is ± 1 pS though this value will vary depending on the experimental error in both test runs.

When comparing devices, in addition to the DI matching, the gate electrodes must also be examined under a microscope to ensure an electrode in approximately the same location (within 100 μm of each other's location) exist on both devices. This is due to a report previously demonstrating that location of the gate with respect to the grounded nanochannel will have an effect on the resulting measured net current during runs where a gate voltage is applied (M. Fuest, et al., 2015). If both of these requirements are met, the devices can be used for testing and are considered to have equivalent geometry.

With DI matched devices of equivalent geometry, a series of tests were conducted with a constant DC axial potential of 3 V applied while the gate electrode was varied. Of the collected data, 2 V DC or 2 V_{RMS} AC was selected as the gate voltage to form a representative study from though all trends seen in the 2 V case were present throughout the data set. In part, this voltage was selected for the abundance of data related to this voltage in existing literature for DC drive gated nanofluidic field effect devices. Current modulation was selected as the parameter of interest. For the DC case, current modulation refers to the maximum difference between the negative and positive cases of a given gate voltage. For the AC cases, current modulation refers to the maximum and minimum values within a single RMS matched gate voltage. In Table 1, the current modulation between cases is shown. Here, it can be clearly shown that even for the small frequency range examined in this work, there is a large dependence of current modulation on applied AC signal frequency. Additionally, it can be seen that in all AC cases, the current modulation was higher than for the DC case.

Adviser: Shaurya Prakash
Collaborators: Marie Fuest and Kyle Wellmerling

Table 1: Current modulation vs. waveform. These results are from the 2 V_{RMS} matched case where the current modulation is the difference between the peak measured current in each case and the frequency and waveform refer to the applied potential. For the DC current modulation, the difference between the 2 V and -2 V case is shown. All AC cases showed increased current modulation over the DC case and current modulation was shown to increase with current. A constant 3 V DC axial potential was applied in all cases while only the gate electrode potential was altered to have the AC signal.

Waveform	Frequency	Current Modulation
DC	-	1.2 pA
Sine	0.1 Hz	20.1 pA
Sine	0.3 Hz	28.3 pA
Sine	0.5 Hz	38.4 pA

In addition to the first demonstration of an AC signal used to drive ionic transport through a single gated nanofluidic device, conclusions from this study revealed the AC signals showing an order of magnitude higher current modulation than in the DC case (as seen in Table 1). The implications of this work would be the indication lower applied gate voltages to drive equivalent ionic transport in nanochannels with AC signals. This could allow water desalination systems based off this technology to remove ionic contaminates at lower voltages resulting in overall lower power consumption working toward the eventual goal of a handheld desalination unit.

With this feasibility study, future work will go on to examine the effect of frequency over a larger, several orders of magnitude range, the effect of alternate waveforms such as square, sawtooth, and triangular waveforms, the effect of electrolyte valence with a calcium chloride based comparison, and the effect of electrolyte concentration on this behavior. Additionally, for the expanded work, an investigation in to the total charge through the device and an explanation for the results backed up with numerical models is currently being pursued. It is clear interesting effects are taking place and further investigation will be needed to fully understand the mechanisms leading to this behavior though it is suspected that concentration changes inside the nanochannels

Adviser: Shaurya Prakash
Collaborators: Marie Fuest and Kyle Wellmerling

and the charging and discharging cycles of the electric double layer have at least some effect on the overwhelmingly clear difference between the AC and DC signals seen here.

References

Ai, Y., Zhang, B., & Qian, S. (2010). Field Effect Regulation of DNA Translocation through a Nanopore. *Analytical Chemistry, 82*, 8217-8225.

Ajdari, A. (2000). Pumping liquids using asymmetric electrode arrays. *Phys. Rev. E, 45*.

Bazant, M. Z., & Ben, Y. (2006). Theoretical prediction of fast 3D AC electro-osmotic pumps. *Lab on a Chip, 6*, 1455-1461.

Bazant, M. Z., Kilic, M. S., Storey, B. D., & Ajdari, A. (2009). Towards an understanding of induced-charge electrokinetics at large applied voltages in concentrated solutions. *Advances in Colloid and Interface Science*(152), 48-88.

Bazant, M. Z., Urbanski, J. P., Levitan, J. A., Subramanian, K., Kilic, M. S., Jones, A., & Thorsen, T. (2007). *ELECTROLYTE DEPEDENCE OF AC ELECTRO-OSMOSIS*. Paper presented at the Proceedings of 11th International Conference on Miniaturized Systems for Chemistry and Life Sciences (MicroTAS).

Brown, A. B. D., Smith, C. G., & Rennie, A. R. (2000). Pumping of water with ac electric fields applied to asymmetric pairs of microelectrodes. *PHYSICAL REVIEW E, 63*.

Duan, C., & Majumdar, A. (2010). Anomalous ion transport in 2 nm hydrophilic nanochannels. *Natue nanotechnology, 5*, 848-852.

Duan, R., Xia, F., & Jiang, L. (2013). Constructing Tunable Nanopores and Their Application in Drug Delivery. *ACS Nano, 7*(10), 8344-8349.

Fuest, M., Boone, C., Rangharajan, K. K., Conlisk, A. T., & Prakash, S. (2015). A Three-State Nanofluidic Field Effect Switch. *Nano Letters*. Retrieved from doi:10.1021/nl504236

Fuest, M., Boone, C., Rangharajan, K. K., Conlisk, A. T., & Prakash, S. (2016). Cation Dependent Surface Charge Regulation in Gated Nanofluidic Devices. *Applied Physics Letters, (In Review)*.

Fuest, M. J. (2016). *Active Electrokinetic Transport Control in a Nanofluidic Device with Embedded Surface Electrodes*. PhD Active Electrokinetic Transport Control in a Nanofluidic Device with Embedded Surface Electrodes, The Ohio State University, Columbus.

Garcia-Sanchez, P., Ramos, A., Green, N. G., & Morgan, H. (2006). Experiments on AC electrokinetic pumping of liquids using arrays of microelectrodes. *IEEE Transactions on Dielectrics and Electrical Insulation, 13*(3), 670 - 677.

Guan, W., Fan, R., & Reed, M. A. (2011). Field-effect reconfigurable nanofluidic ionic diodes. *Nature Communications 2*.

Guan, W., & Reed, M. A. (2012). Electric Field Modulation of the Membrane Potential in Solid-State Ion Channels. *Nano letters, 12*(12), 6441–6447. doi: 10.1021/nl303820a

Hille, B. (2001). *Ion Channels of Excitable Membranes* (Third ed.). Seattle: The University of Washington.

Howorka, S., & Siwy, Z. (2009). Nanopore analytics: sensing of single molecules. *Chemical Society Reviews*(8), 2360-2384.

Huang, C.-C., Bazant, M. Z., & Thorsen, T. (2009). Ultrafast high-pressure AC electro-osmotic pumps for portable biomedical microfluidics. *Lab on a Chip, 10*, 80-85.

Huo, X., Guo, W., & Jiang, L. (2011). Biomimetric smart nanopores and nanochannels. *Chemical Society Reviews, 40*, 2385-2401.

Karnik, R., Fan, R., Yue, M., Li, D., Yang, P., & Majumdar, A. (2005). Electrostatic Control of Ions and Molecules in Nanofluidic Transistors. *Nano letters, 5*(5), 943-948.

Kim, S. J., Ko, S. H., Kang, K. H., & Han, J. (2010). Direct seawater desalination by ion concentration polarization. *Nature Nanotechnology, 5*, 297 - 301.

Adviser: Shaurya Prakash
Collaborators: Marie Fuest and Kyle Wellmerling

Lastochkin, D., Zhou, R., Wang, P., Ben, Y., & Chang, H.-C. (2004). Electrokinetic micropump and micromixer design based on acac faradaic polarization. *Journal of Applied Physics, 96*(3).

Liu, M., Zhang, H., Li, K., Heng, L., Wang, S., Tian, Y., & Jiang, L. (2014). A Bio-inspired Potassium and pH Responsive Double Gated Nanochannel. *Advanced Functional Materials, 25*, 421-426.

Ramos, A., González, A., Castellanos, A., Green, N. G., & Morgan, H. (2003). Pumping of liquids with ac voltages applied to asymmetric pairs of microelectrodes. *Phys. Rev. E, 67*.

Ramos, A., Morgan, H., Green, N. G., & Castellanos, A. (1999). AC Electric-Field-Induced Fluid Flow in Microelectrodes. *Journal of Colloid Interface Science, 2*(217), 420-422.

Shannon, M. A. (2010). Water desalination: Fresh for less. *Nature Nanotechnology, 5*, 248 - 250.

Siria, A., Poncharal, P., Biance, A.-L., Fulcrand, R., Blase, X., Purcell, S. T., & Bocquet, L. (2013). Giant osmotic energy conversion measured in a single transmembrane boron nitride nanotube. *Nature*(494), 455–458.

Soni, G., Squires, T. M., & Meinhart, C. D. (2007). *NONLINEAR PHENOMENA IN INDUCED-CHARGEELECTROOSMOSIS: A NUMERICAL AND EXPERIMENTAL INVESTIGATION*. Paper presented at the The 11th International Conference on Miniaturized Systems for Chemistry and Life Sciences, MicroTAS 2007, Paris, France.

Sparreboom, W., Cucu, C. F., Eijkel, J. C. T., & Berg, A. v. d. (2008). *ION PUMPING IN NANOCHANNELS USING AN ASYMMETRIC ELECTRODE ARRAY*. Paper presented at the Twelfth International Conference on Miniaturized Systems for Chemistry and Life Sciences, San Diego, CA, United States.

Sparreboom, W., van den Berg, A., & Eijkel, J. C. T. (2010). Transport in nanofluidic systems: a review of theory and applications. *New Journal of Physics, 12*.

Stein, D., Kruithof, M., & Dekker, C. (2004). Surface Charge Governed Ion Transport in Nanofluidic Channels. *Physical Review Letters, 93*(3), 035901 035901-035904.

Storey, B. D., Edwards, L. R., Kilic, M. S., & Bazant, M. Z. (2008). Steric effects on ac electro-osmosis in dilute electrolytes. *PHYSICAL REVIEW E*(77).

Adviser: Shaurya Prakash
Collaborators: Marie Fuest and Kyle Wellmerling

Studer, V., Pépin, A., Chen, Y., & Ajdari, A. (2004). An integrated AC electrokinetic pump in a microfluidic loop for fast and tunable flow control. *The Analyst, 129*, 944-949.

Urbanski, J. P., Thorsen, T., Levitan, J. A., & Bazant, M. Z. (2006). Fast ac electro-osmotic micropumps with nonplanar electrodes. *Applied Physics Letters, 89*. doi: doi: 10.1063/1.2358823

van den Beld, W. T. E., Sparreboom, W., van den Berg, A., & Eijkel, J. C. T. (2014, 26-30 January 2014). *FREQUENCY DEPENDENT AC ELECTROOSMOTIC FLOW IN NANOCHANNELS.* Paper presented at the Technical Digest of the 27th IEEE International Conference on Micro Electro Mechanical Systems, MEMS 2014, San Francisco, CA, United States.

van der Wouden, E. J., Hermes, D. C., Gardeniers, J. G., & van den Berg, A. (2006). Directional flow induced by synchronized longitudinal and zeta-potential controlling AC-electrical fields. *Lab on a Chip, 6*(10), 1300-1305.

Wei, R., Gatterdam, V., Wieneke, R., Tampé, R., & Rant, U. (2012). Stochastic sensing of proteins with receptor-modified solid-state nanopores. *Nature Nanotechnology, 7*, 257–263. doi: doi:10.1038/nnano.2012.24

Xia, D., Yan, J., & Hou, S. (2012). Fabrication of Nanofluidic Biochips with Nanochannels for Applications in DNA Analysis. *Small, 8*(18), 2787–2801.

Yang, H., Jiang, H., & Ramos, A. (2009). AC electrokinetic pumping on symmetric electrode arrays. *Microfluid Nanofluid, 7*, 767-772.

Adviser: Shaurya Prakash
Collaborators: Marie Fuest and Kyle Wellmerling